Ind. J. Pharm. Edu. Res., 2025; 59(4):1501-1510.
https://www.ijper.org

Original Article

Atorvastatin Ameliorates Neuroinflammatory Response in Experimental Intracerebral Hemorrhage Rats through the GSK-3β/β-Catenin Pathway

Jing Zhao, Mei Li, Lingling Zhang, Qi Zhang*

Department of Neurology, Nantong RICH Hospital, Nantong, Jiangsu, CHINA.

ABSTRACT

Objectives: This study aimed to elucidate influence of Atorvastatin (ATV) on the neuroinflammatory response in experimental Intracerebral Hemorrhage (ICH) through the GSK-3β/β-catenin Signaling Pathway (SPW). **Materials and Methods:** Forty-five rats were randomly rolled into Sham, ICH (established using the Fredrik methodology) and ATV intervention (ICH model+10 mg/kg ATV) groups, each comprising 15 rats. Neurological deficits in rats were assessed using the Garcia methodology. Brain Water Content (BWC) was measured via wet-dry methodology. Nissl staining was conducted to observe Brain Tissue (BT) histological changes and count undamaged neurons. Expression Levels (ELs) of β-catenin, GSK-3β and p-GSK-3β in BT were detected. Levels of Inflammatory Factors (IFs) Tumor Necrosis Factor (TNF)-α, Interleukin (IL)-1β and IL-6 in rat cerebrospinal fluid were measured. **Results:** Relative to Sham group, ICH group exhibited decreased postoperative neurological behavior scores, β-catenin gene mRNA ELs and β-catenin protein levels, along with a reduction in the number of intact neurons ($p<0.05$). BT BWC, GSK-3β gene levels, p-GSK-3β and GSK-3β protein ELs were greatly increased, that is, $p<0.05$, while IL-6, IL-1β and TNF-α in cerebrospinal fluid were markedly elevated ($p<0.05$). In comparison to ICH group, ATV group showed increased neurological behavior scores, β-catenin gene mRNA levels and β-catenin protein levels, with an increase in the number of intact neurons ($p<0.05$). Moreover, BWC, GSK-3β gene mRNA ELs, p-GSK-3β and GSK-3β protein ELs, as well as IFs, were notably decreased ($p<0.05$). **Conclusion:** ATV, through regulation of the GSK-3β/β-catenin SPW, inhibits inflammatory reactions and cellular damage, thereby ameliorating neurological dysfunction and neuroinflammatory responses in experimental ICH rats.

Keywords: Atorvastatin, Experimental cerebral hemorrhage, Gsk-3β/β-catenin signaling pathway, Inflammatory reaction, Neuroprotection.

Correspondence:
Mr. Qi Zhang
Department of Neurology, Nantong RICH Hospital, Nantong-226000, Jiangsu, CHINA.
Email: zhangqi88948@yeah.net

Received: 06-12-2024;
Revised: 24-02-2025;
Accepted: 16-06-2025.

INTRODUCTION

The occurrence and progression of Intracerebral Hemorrhage (ICH) involve various primary pathologies such as vascular abnormalities, hypertension and hematologic disorders, as well as secondary injury processes.[1] Following ICH onset, blood leakage into Brain Tissues (BT) leads to local vascular rupture, hematoma formation and direct damage to surrounding neurons, triggering a cascade of inflammatory responses.[2] While inflammation is the body's protective response, it can exacerbate neural damage and lead to inflammatory cell death.[3] Improper regulation of inflammation may worsen BT damage, impacting patient recovery. GSK-3β is involved in regulating various life processes and closely associated with neuronal injury.[4] Recent studies identified GSK-3β as playing a crucial role in inflammation, with its activation being a key requirement to produce Inflammatory Factors (IFs).[5] However, the regulatory mechanisms of GSK-3β in neuroinflammatory response following ICH remain incompletely understood.

Atorvastatin (ATV) belongs to the new generation of drugs targeting this enzyme. By inhibiting 3-Hydroxy-3-Methylglutaryl Coenzyme A (HMG-CoA) reductase, ATV reduces cholesterol synthesis. It can exert various biological effects, including cholesterol reduction, anti-inflammatory, antioxidative, immunomodulatory and neuroprotective properties.[6-8] As a commonly used lipid-lowering medication, ATV offers advantages of high safety and good tolerability, primarily indicated for treating conditions such as hypercholesterolemia, hyperlipidemia and coronary heart disease. ATV significantly reduces blood viscosity, alleviating symptoms of hemorrhagic brain injury.[9] Additionally, ATV possesses vascular protective effects, improving vascular function, maintaining blood-brain

DOI: 10.5530/ijper.20250529

barrier permeability, inhibiting brain edema, promoting BT reperfusion, mitigating brain damage and inflammatory responses, alleviating post-hemorrhagic cerebral vasospasm, thus aiding in the recovery from neurological disorders.[10] The anti-inflammatory mechanism of ATV primarily involves attenuating the chemotaxis and aggregation of inflammatory cells into plaques and inhibiting the Expression Levels (ELs) of soluble intercellular adhesion molecules and metalloproteinases in macrophages.[11] Recent studies indicated that ATV can inhibit GSK-3β activity, thereby influencing various cellular Signaling Pathways (SPWs) and regulating various biological processes.[12,13] It is evident that ATV is not only a lipid-lowering medication but also a potential therapeutic agent for neuroinflammatory diseases. Its mechanism of improving neuroinflammatory response by modulating the GSK-3β-β-catenin SPW warrants further investigation. Moreover, its role in the neuroinflammatory response following ICH remains incompletely understood and requires further elucidation.

Hence, mechanism of ATV in experimental ICH rats was demonstrated, particularly whether it improved neuroinflammatory response by modulating the GSK-3β/β-catenin SPW. The goal was to elucidate the mechanism of ATV in treating ICH, providing a theoretical basis for developing novel therapeutic strategies to enhance prognosis and quality of life of ICH patients.

MATERIALS AND METHODS

Animals and grouping

45 healthy Sprague-Dawley rats (male, 9-12 weeks old, 270~331 g) were selected from Chengdu Dashuo Experimental Animal Center, China. Mice were accommodated in groups of five in controlled experimental animal rooms with specific pathogen-free conditions. The rooms were kept at a temperature of 25±°C, around 55% relative humidity and operated on a 12-hr light-dark cycle. Animals had unrestricted access to food and water. Animal protocols were sanctioned by Experimental Animal Management Committee and followed approved guidelines.

After a 2-week acclimatization, rats were rolled into Sham, ICH and ATV groups (each n=15). Rats in the Sham and ICH groups were administered 2 mL of 0.9% saline solution by gavage, while rats in ATV group received oral gavage of 10 mg/kg ATV (Pfizer Inc., USA) for intervention.

Establishment of ICH model

The ICH model in rats was prepared using the Fredrik methodology,[14] with specific procedures as follows. 30 mg/kg of 1% pentobarbital sodium were adopted to anesthetize animals via intraperitoneal injection (Shanghai Yanjin Biological Technology Co., Ltd., China). Following successful anesthesia, arterial blood pressure was measured by catheter insertion into right femoral artery and right basal ganglia region were injected with 50 μL blood. Animals were then placed in a stereotaxic apparatus with their skull exposed. A burr hole was drilled on the right side as against bregma: anterior-posterior 0.2 mM, lateral 5.5 mM and depth 3.5 mM. Using a microsyringe, right basal ganglia (located at anterior-posterior 0.2 mm, lateral 5.5 mM and depth 6 mM) were injected with 50 μL arterial blood. During the injection, 10 μL of blood was first injected very slowly, followed by a 5 min pause, after which the needle was moved down to a depth of 5.8 mM and the remaining 40 μL of blood was injected slowly. The entire injection process lasted for 30 min. After injection, the syringe was slowly withdrawn, the cranial incision was closed, and the surgical area was routinely disinfected. The skin was sutured, and rats were maintained on a regular diet. In ATV group, rats were orally administered 10 mg/kg of ATV by gavage 2 hr after surgery, once daily for 7 consecutive days. Rats in the Sham and ICH groups were orally administered 2 mL of 0.9% saline solution by gavage, once daily for 7 consecutive days.

Neurological dysfunction score

Neurological deficits in each group of rats were assessed using the Garcia methodology[15] at 12 hr, 24 hr, 48 hr, 96 hr and 7 days postoperatively. This methodology comprises six basic tests: spontaneous activity, symmetry of movements, tactile startle response, wire grip test, symmetry of forelimbs and tactile response of both sides of the trunk. Each test was scored on a specific scale: spontaneous activity (0-3 points), symmetry of movements (0-3 points), tactile startle response (1-3 points), wire grip test (1-3 points), symmetry of forelimbs (0-3 points) and tactile response of both sides of the trunk (1-3 points). The individual scores from these tests were combined to calculate a total score of 3-18 points. A lower total score suggested more pronounced neurological deficits.

Determination of water content in BT

BT Water Content (BWC) was measured using the wet-dry methodology.[16] At 24 hr, 36 hr and 72 hr postoperatively, all rats were euthanized by decapitation under anesthesia with 30 mg/kg of 1% pentobarbital sodium. After decapitation, brains were rapidly removed on an ice-cold plate and approximately 100 mg of BT surrounding the hematoma was collected. The wet weight of the samples was accurately measured using a precision electronic balance (Shanghai Tianping Instrument Factory, China). Subsequently, samples were placed in a constant temperature oven at 100°C for 48 hr to determine their dry weight. The BWC was then calculated.

Nissl staining of BT

Rat brain basal ganglia tissue samples were collected, fixed, embedded and processed into routine paraffin sections using a tissue slicer (Leitz, Germany). After paraffinization, sections were immediately immersed in xylene I and xylene II (Wuhan Canos Technology Co., Ltd., China) for 20 min each. They were

then dehydrated in a series of various concentrations of ethanol (China National Pharmaceutical Group Chemical Reagent Co., Ltd., China) (100% ethanol I, 100% ethanol II, 95% ethanol I, 95% ethanol II, 90%, 80% and 70% ethanol), with each immersion lasting 5 min, followed by immersion in double distilled water for 5 min. Samples were stained in containers containing toluidine violet solution (Dingzhou Bioseth Biological Technology Co., Ltd., China) for 30 min in an incubator (37°C), examined under a microscope (Olympus Corporation, Japan) to check staining outcomes, rinsed with tap water until a bluing effect was observed and dehydrated again in different concentrations of ethanol (70%, 80%, 90% ethanol, as well as 95% ethanol I, 95% ethanol II, 100% ethanol I and 100% ethanol II) for 5 min each. Finally, samples were sequentially placed in xylene I and II for 5 min each for transparent treatment, fixed with neutral gum (Shanghai Specimen Model Factory, China) and observed under a microscope. Neurons around the hematoma were selected and at 40×magnification, five random high-power fields were chosen to visualize neurons with intact nuclei. Neurons with clear and undamaged nuclei were counted and the mean number of positive cells counted in five fields was taken as count of undamaged neurons.

Real-time fluorescence quantitative PCR

mRNA ELs of GSK-3β/β-catenin genes in BTs of each group were detected using qRT-qPCR. BTs within a 3 mm range around the lesion in rats were isolated and 100 mg of BT was collected. Total RNA from the BTs was extracted employing TRIzol methodology. RNA purity and concentration were scored utilizing a Qubit Fluorometer (Thermo Fisher, USA) and agarose gel electrophoresis. Reverse transcription was performed with a kit (Beijing Solarbio Technology Co., Ltd., China) with 20 μL reaction volume, containing 1 μg RNA, 2 μL 10 mM dNTP, 4 μL 5× Buffer, 1 μL Oligo (dT) and 0.5 μL reverse transcriptase. The reverse transcription program consisted of incubation at 42°C for 60 min and 75°C for 10 min. Subsequently, 1 μL of reverse transcription product served as a template for amplification using SYBR Green Master Mix (TaKaRa, Japan). Amplification reaction included initial denaturation at 95°C for 3 min, 30 cycles of denaturation at 95°C for 10 sec, annealing at 55°C for 34 sec. GAPDH and were used as reference genes to analyze the ELs of GSK-3β gene in BTs. Each reaction was performed in triplicate utilizing at 60°C for 30 sec (30 cycles). Relative EL of GSK-3β gene in BTs was calculated via $2^{-\Delta\Delta ct}$ method. Primer sequences for amplifying the GSK-3β and β-catenin genes, as well as GAPDH, are detailed in Table 1. All primer sequences were custom-designed and synthesized.

Western Blotting

BTs within a 3 mm range around the lesion in rats were dissected and 100 mg of BT was weighed. The rat BT was placed in a homogenizer and thoroughly minced. Then, 1 mL of pre-prepared lysis buffer (radioimmuno precipitation assay protein lysis buffer: protease inhibitor phenylmethylsulfonyl fluoride=1:100) was applied for grinding. Mixture was chilled on ice for 30 min, then centrifugated at 12,000 rpm for 20 min at 4°C to isolate total protein extract. Protein concentration was determined utilizing BCA assay (Shanghai Enzyme-linked Biotechnology Co., Ltd., China). Proteins were denatured by boiling in water for 10 min and sodium dodecyl sulphate-polyacrylamide gel electrophoresis gel electrophoresis (10% separating gel, 5% stacking gel) was utilized to separate them. Finally, proteins were transferred onto polyvinylidene fluoride membranes via a wet transfer methodology at a constant current of 250 mA for 60-90 min, which were blocked with 5% skim milk for 1 hr and then incubated overnight at 4°C with appropriately diluted primary Antibodies (Abs): rabbit anti-rat p-GSK-3β (1:200), GSK-3β (1:200), β-catenin (1:400) and β-actin Abs (1:500) (all sourced from Abcam, UK). After washing thrice with TBST for 10 min each, horseradish peroxidase-conjugated secondary Abs (1:10,000) (Shanghai Rebiosci Biotechnology Co., Ltd., China) was utilized to incubate membranes at 25°C for 2 hr. Following another three washes with TBST, membranes were incubated with a chromogenic substrate and automatic exposure was performed using a gel imaging system. Under grayscale values, protein ELs of β-catenin, GSK-3β and p-GSK-3β were acquired.

ELISA

Prior to euthanasia, Cerebrospinal Fluid (CSF) samples were collected from rats. IFs levels in rat CSF were acquired utilizing ELISA kits (Shanghai Enzyme-linked Biotechnology Co., Ltd., China). Diluted protein standards and sample diluent were added to the enzyme-labeled wells, followed by the addition of blocking solution. After incubation with rabbit anti-rat IL-6, IL-1β and TNF-α Abs (1:100) and goat anti-rabbit secondary Abs (1:1000), each well was incubated with 100 μL of chromogenic substrate. Subsequently, plate was incubated in the dark for 10 min and absorbance of each well was promptly measured at 450 nm via ELISA reader within 5 min after terminating the chromogenic reaction.

Table 1: Primer sequences amplified by qRT-PCR.

Gene	Forward primers	Reverse primer
GSK-3β	5'- TACCCATACGATGTTCCAGAT-3'	5'- CCCTGC-CCAGGAGTTGCCAC-3'
β-catenin	5'-GAAGATCAAGATCATTGCTCCT-3'	5'- ACTCCTGCTTGCTGATCCA-3'
GAPDH	5'-AGTTCAACGGCACAGTCAAG-3'	5'-CAGCCTTCTCCATGGTGGTG-3'

Statistical processing

Statistical analysis of the experimental data was conducted using *SPSS 19.0*. The continuous variables were normally distributed with homogeneity of variance and were expressed as mean±standard deviation ($\bar{x}\pm s$). Comparisons among multiple groups were performed using one-way analysis of variance, while pairwise comparisons between groups utilized the LSD test. A *p*-value of less than 0.05 was considered statistically significant.

RESULTS

Neurological dysfunction score: Preoperatively, all rats exhibited normal neurological behavior. Rats in Sham group showed neglectable characteristics of neurological dysfunction postoperatively, with neurological function scores ranging from 17 to 19. Rats in ICH group exhibited pronounced neurological deficits postoperatively, with neurological function scores ranging from 8 to 12, reaching the lowest point at 24 hr, characterized by mild or absent movement of the left limbs and inability to climb. Over time, neurological deficits in ICH group gradually improved, as indicated by a progressive increase in neurological function scores. Neurological deficits in ATV group were alleviated relative to ICH group. The results of the LSD test indicated that, relative to Sham group, neurological scores in ICH group were greatly decreased at 12 hr, 24 hr, 48 hr, 96 hr and 7 days postoperatively ($p<0.05$). Furthermore, neurological scores in ATV group were drastically increased at 12 hr, 24 hr, 48 hr, 96 hr and 7 days postoperatively versus ICH group, that is, $p<0.05$ (Figure 1).

Dynamic changes in BT water content

Postoperatively, the BT BWC in ICH group rats exhibited a trend of initial elevate followed by a decline, with the highest BWC content reached at 36 hr postoperatively. Similarly, the BT BWC in ATV group rats also showed a trend of initial elevate followed by a decline, with the highest BWC content reached at 36 hr postoperatively. Both ICH group and ATV group showed notably increased BT BWC versus Sham group, that is, $p<0.05$. Moreover, BT BWC in ATV group was greatly decreased relative to ICH group, that is, $p<0.05$. No marked difference was indicated in BT BWC between Sham and ATV groups, that is, $p>0.05$ (Figure 2).

Nissl staining of BT

In the Sham group, neuronal cell morphology appeared normal, with slight reduction in the number of Nissl bodies observed. In contrast, neuronal cells in ICH group exhibited diverse morphologies, decreased in number and correspondingly reduced in size, with a drastic decline in the number of Nissl bodies, nuclear fragmentation and pronounced BT swelling and necrosis. Compared to ICH group, ATV group showed a reduction in damaged neuronal cell count, an increase in the number of Nissl bodies and some improvement in nuclear fragmentation, BT swelling and necrosis; however, there still existed a certain degree of neuronal cell damage compared to Sham group (Figure 3A).

The number of undamaged neurons in the Sham group remained stable over different time periods. The number of undamaged neurons in ICH group substantially decreased at different time points versus Sham group, with the difference between ICH and Sham groups increasing with postoperative time. Specifically, at 12 hr, 36 hr and 72 hr postoperatively, the number of undamaged neurons in ICH group was markedly reduced versus Sham group, that is, $p<0.05$. Furthermore, in Figure 3B, a marked increase in the number of undamaged neurons can be observed in ATV group at 12 hr, 36 hr and 72 hr postoperatively versus ICH group, that is, $p<0.05$.

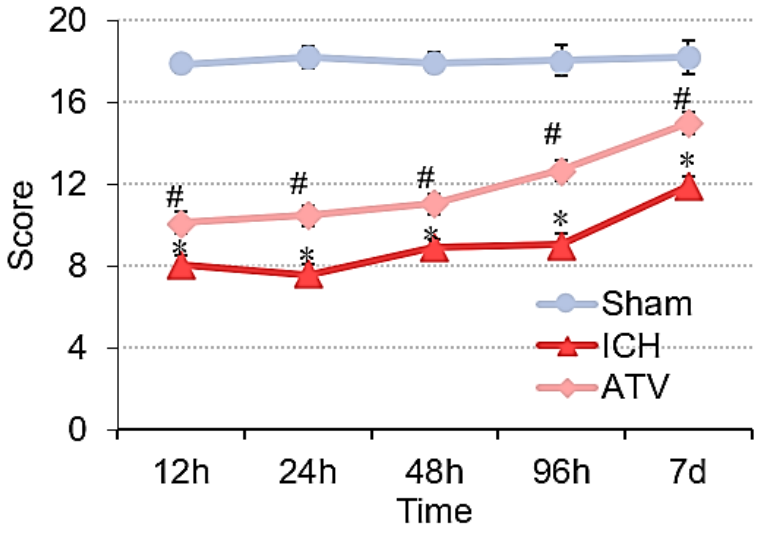

Figure 1: Comparison of neurobehavioral scoring among different groups at postoperative 12 hr, 24 hr, 48 hr, 96 hr and 7 days. Denotes $p<0.05$ vs. Sham group; # denotes $p<0.05$ vs. ICH group.

Analysis of EL of GSK-3β/β-catenin SPW in BT: Results of GSK-3β and β-catenin gene ELs in BT revealed that, relative to Sham group, the mRNA ELs of GSK-3β gene in ICH group were notably elevated at 12 hr, 36 hr and 72 hr postoperatively, that is, $p<0.05$, while mRNA ELs of the β-catenin gene were greatly reduced, that is, $p<0.05$. Moreover, with prolonged time, the reduction in β-catenin gene mRNA ELs in ICH group became more pronounced. The mRNA ELs of the GSK-3β/β-catenin genes showed inconsiderable differences between various time points in ICH group, that is, $p>0.05$. The mRNA ELs of the GSK-3β gene in ATV group were greatly decreased at various postoperative time points versus ICH group, that is, $p<0.05$, while the mRNA ELs of the β-catenin gene were drastically elevated, that is, $p<0.05$. Nevertheless, in Figure 4A-B, neglectable differences between ATV and Sham groups were observed, that is, $p>0.05$.

Relative to Sham group, protein ELs of p-GSK-3β and GSK-3β were substantially elevated in ICH group, that is, $p<0.05$, whereas protein ELs of p-GSK-3β and GSK-3β were greatly decreased in ATV group versus ICH group, that is, $p<0.05$. Protein ELs of p-GSK-3β and GSK-3β differed slightly between ATV group and Sham, that is, $p>0.05$. Protein ELs of β-catenin were greatly reduced in ICH group versus Sham, that is, $p<0.05$. Conversely, relative to ICH group, ATV group exhibited a drastic increase in the protein ELs of β-catenin, that is, $p<0.05$. However, in Figure 4C-F, the protein ELs of β-catenin differed inconsiderably between ATV group and Sham group, that is, $p>0.05$.

ELISA outcomes

Results of ELISA testing for ELs of IFs in CSF showed that, over time, IFs levels in CSF of Sham group remained stable. In contrast, these levels in the CSF of ICH group exhibited a notable upward trend over time. These levels in CSF of ICH group were intermediate between those of the Sham and ICH groups, showing an increasing trend over time, albeit not significant. These levels in the CSF of ICH group were greatly elevated relative to Sham group, that is, $p<0.05$. Furthermore, these levels in CSF of ATV group declined notably relative to ICH group, that is, $p<0.05$. Nevertheless, in Figure 5, these levels in CSF differed slightly between ATV group and Sham group, that is, $p>0.05$.

DISCUSSION

This work investigated the effects of ATV on damaged neurons, apoptosis of surrounding cells and the ELs of molecules related to GSK-3β/β-catenin SPW under a rat model of ICH. The aim was to discuss the mechanism of ATV in treating experimental ICH and its impact on GSK-3β/β-catenin SPW. The results showed marked improvements in neurobehavioral scores, decreased ELs of the β-catenin gene and protein, reduced numbers of undamaged neurons, decreased BT water content and drastically increased ELs of the GSK-3β gene and protein, along with a notable increase in IF levels in the cerebrospinal fluid after ICH. Following ATV intervention, ICH group exhibited improved neurobehavioral scores, increased numbers of undamaged neurons, decreased BT water content, as well as regulation of the GSK-3β/β-catenin SPW and reduced IF levels.

The present study utilized autologous blood injection to establish the ICH model, which effectively reproduces pathological processes such as brain edema formation and tissue pathological reactions observed in human ICH.[17,18] Behavioral characteristics observed in ICH animals include reduced limb activity, decreased

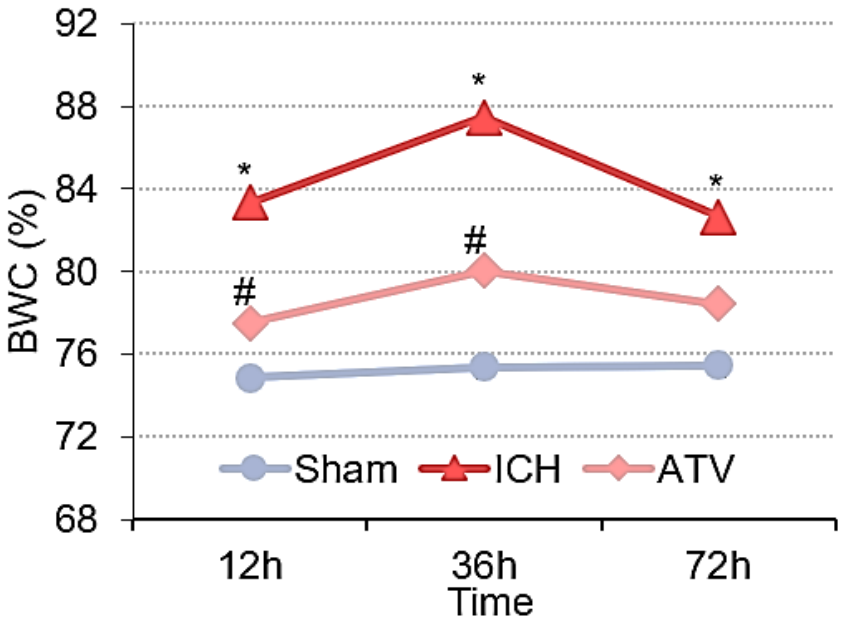

Figure 2: Comparison of brain tissue water content at postoperative 12 hr, 36 hr and 72 hr among different groups. Denotes $p<0.05$ vs. Sham group; # denotes $p<0.05$ vs. ICH group.

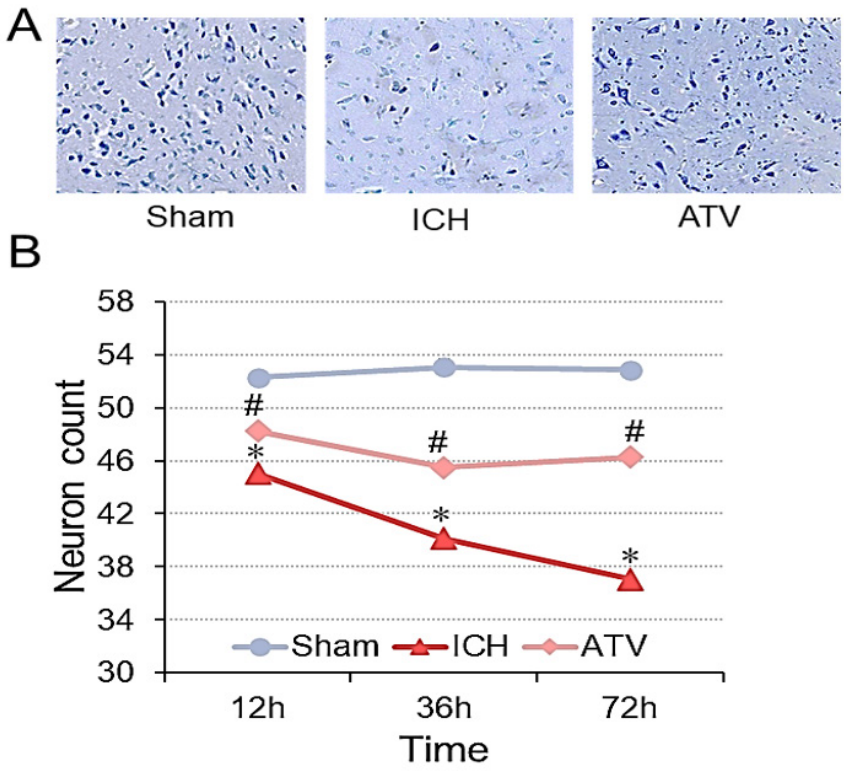

Figure 3: Nissl staining of brain tissue at postoperative 12 hr, 36 hr and 72 hr among different groups. A: Nissl staining (× 400); B: number of undamaged neurons. Denotes $p<0.05$ vs. Sham group; # denotes $p<0.05$ vs. ICH group.

spontaneous movement and loss of limb symmetry.[19] The results revealed that rats in ICH group exhibited notable neurobehavioral impairments postoperatively versus Sham group, with a notable decrease in neurobehavioral scores, particularly reaching a nadir at 24 hr. This manifested as mild or absent movement in the left limbs and an inability to climb. Over time, there was some alleviation of neurobehavioral impairmenourts, but the scores remained lower than those of Sham group, consistent with findings from previous studies.[20,21] These studies report improvements in neurobehavior across different models, indicating that over time, compromised neurological function may partially recover. In contrast to ICH group, rats in ATV group showed an observable improvement in neurobehavioral scores, indicating a positive effect of ATV on ameliorating neurobehavioral impairments. The above study indicated that after the establishment of the ICH model, rats exhibited notable neurofunctional impairments, which gradually alleviated over time. This phenomenon can be attributed to the brain's inherent capacity for self-repair, particularly following mild injuries, where neurons and neural networks can restore functionality through reorganization and reconnection.[22] ICH triggers a cascade of inflammatory responses and as inflammation diminishes, the extent of neural tissue damage decreases, leading to an improvement in neurofunction.[23] ATV intervention can partially ameliorate the neurofunctional impairments caused by ICH, as evidenced by a notable increase in neurofunctional scores. These findings support the neuroprotective role of ATV against brain hemorrhage-induced neuronal damage, providing basis for its clinical application in therapy of ICH.

Furthermore, the results revealed a trend of initially increasing and subsequently decreasing BWC postoperatively in both the ICH and ATV groups, reaching its peak at 36 hr after surgery. This fluctuation pattern may reflect the development of BT edema and subsequent recovery processes following ICH. The initial increase could be attributed to inflammatory responses and edema formation in BT, while the subsequent decrease may be associated with alleviation of inflammation and gradual absorption of edema. Both the ICH and ATV groups exhibited a prominent increase in BT BWC versus Sham group, indicating an increase in BT edema following ICH or ATV intervention. This aligns with the notable increase in BT edema observed during ICH. Relative to ICH group, ATV group exhibited a great reduction in BWC, indicating a beneficial effect of ATV intervention in alleviating BT edema. This may be attributed to the anti-inflammatory, neuroprotective and vascular-improving properties of ATV, which could help mitigate the extent of BT edema. BWC refers to the water content in BT, which is crucial for maintaining osmotic balance between intracellular and extracellular environments. Abnormal BT water content, either excessively high or low, may lead to cellular swelling or shrinkage, thus affecting the normal function of neurons.[24] Changes in BWC could influence the speed and efficiency of neural signal transmission. Excessive water content may impede signal transmission between neurons,

thereby affecting cognitive and motor functions.[25] ATV primarily inhibits ischemia-reperfusion-induced neuronal apoptosis by activating the cAMP/PKA/p-CREB/BDNF SPW, thereby mitigating brain injury in neonatal rats.[26] Additionally, some researchers have indicated that ATV can effectively regulate neuroinflammation following traumatic brain injury by altering peripheral leukocyte infiltration and the alternative polarization of microglia/macrophages.[27]

ATV not only participates in neuroprotection by altering peripheral leukocyte infiltration and the alternative polarization of microglia/macrophages, but also exerts its multifaceted protective effects by modulating the GSK-3β/β-catenin SPW to inhibit neuroinflammatory responses.[28] In contrast to Sham group, protein ELs of p-GSK-3β and GSK-3β were notably elevated, while β-catenin protein EL was markedly declined in ICH group. This indicates that ICH may trigger the activation of the GSK-3β SPW, potentially leading to exacerbated neuronal damage and inflammation. The decrease in β-catenin protein expression is associated with neuronal damage and inflammation induced by ICH. In comparison to ICH group, ATV group exhibited a marked decline in protein ELs of p-GSK-3β and GSK-3β, with a considerable increase in β-catenin protein EL. This suggests that ATV intervention may inhibit the activation of the GSK-3β SPW and promote β-catenin SPW activation, thereby contributing to alleviation of neuronal damage and inflammation and ultimately promoting neuroprotection and repair. GSK-3β is a crucial cellular SPW protein that acts in regulating cell cycle, apoptosis and inflammatory responses. In ICH, the increase in p-GSK-3β may reflect the extent of inflammation and cellular damage. Excessive activation of p-GSK-3β may cause neuronal apoptosis and exacerbation of inflammatory responses.[29] GSK-3β, as a critical cellular SPW regulator, plays key roles in cell cycle regulation, inflammatory responses and apoptosis, with its activity regulation being crucial for maintaining normal neural function. In cases of ICH, GSK-3β is typically overactivated, which may lead to neuronal damage and exacerbation of inflammatory responses.[30] Therefore, inhibiting the activity of GSK-3β may help alleviate neuronal damage caused by ICH. β-catenin, a cell adhesion protein and a key molecule in Wnt SPW, participates in cell adhesion, cell SPW and apoptosis. In cases of ICH, the level of β-catenin may be regulated and its activation level may be associated with neuroprotection and repair processes.[31] Decreasing β-catenin levels may affect the ability of neuroprotection and repair, while increasing β-catenin activation

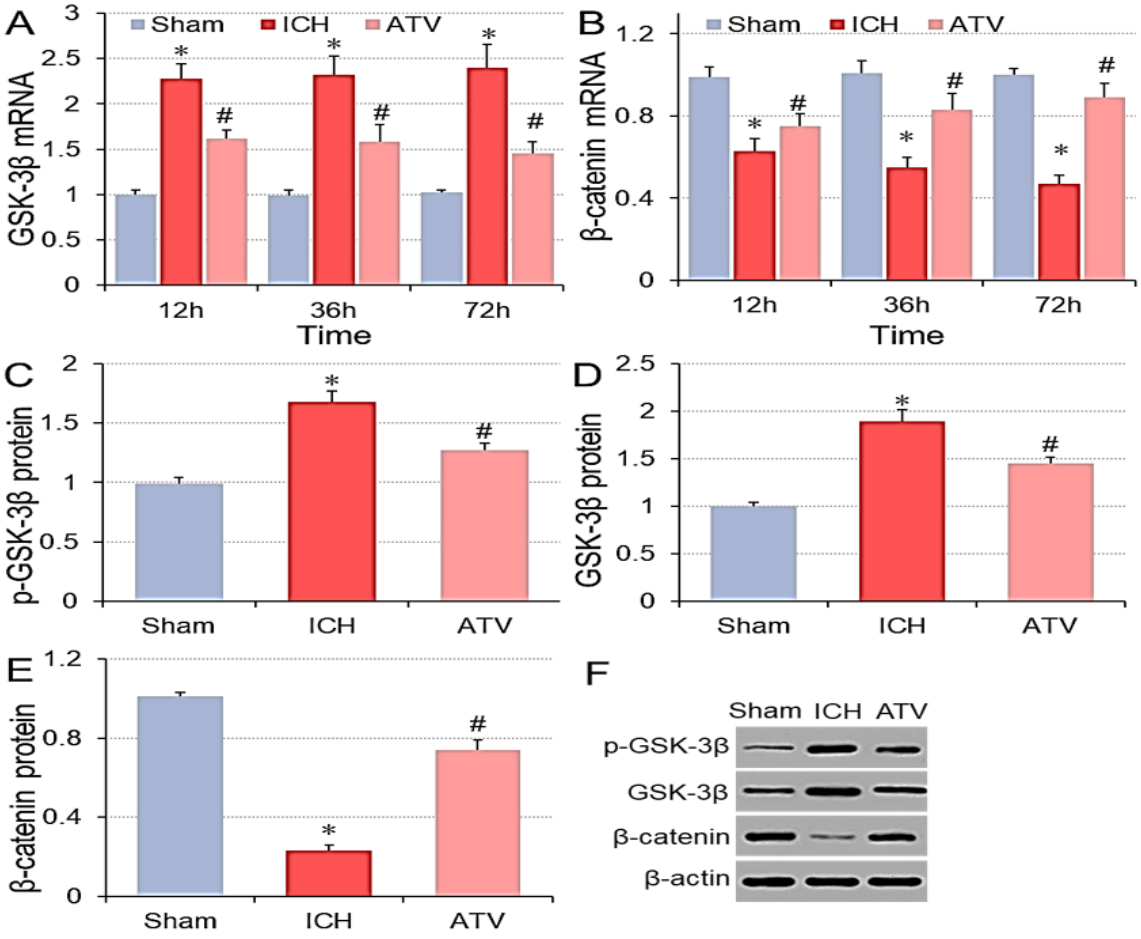

Figure 4: Comparison of gene or protein expression levels of the GSK-3β/β-catenin SPW in brain tissue among different groups post-surgery. A: GSK-3β gene; B: β-catenin gene; C: P-GSK-3β protein; D: GSK-3β protein; E: β-catenin protein; F: western blot. Denotes $p<0.05$ vs. Sham group; # denotes $p<0.05$ vs. ICH group.

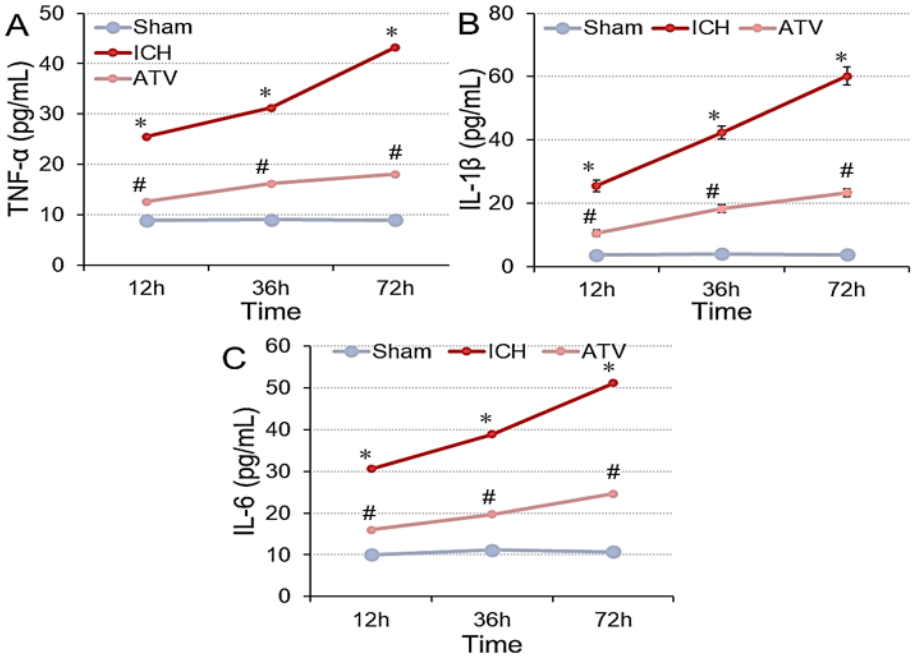

Figure 5: Comparison of cerebrospinal fluid inflammatory factors at postoperative 12 hr, 36 hr and 72 hr among different groups. A: TNF-α; B: IL-1β; C: IL-6. Denotes $p<0.05$ vs. Sham group; # denotes $p<0.05$ vs. ICH group.

may facilitate these processes. The aforementioned studies indicate that changes occur in the ELs of β-catenin, GSK-3β and p-GSK-3β proteins in rat BTs after ICH and ATV intervention can modulate these SPWs, thereby helping to alleviate neuronal damage and promote neuroprotection and repair. ATV exhibits potential application value in patients with cerebral hemorrhage by modulating SPWs associated with neuroprotection and repair. This finding not only offers new perspectives for clinical treatment but also guides future research and drug development efforts.

IFs levels in CSF of ICH group were elevated versus Sham group. These cytokines are crucial regulatory factors in inflammatory responses and their elevation indicates the exacerbation of inflammation induced by cerebral hemorrhage. In contrast, these levels in CSF were greatly declined in ATV group versus ICH group. This suggests that ATV intervention can effectively inhibit release of IFs and alleviate inflammation. In GSK-3β/β-catenin SPW, the increase in TNF-α may lead to GSK-3β activation, thereby affecting β-catenin stability.[32] Specifically, TNF-α action may inhibit β-catenin activation by promoting the phosphorylation of GSK-3β, thereby suppressing its roles in promoting cell proliferation and neuroprotection. IL-1β can promote the activation of GSK-3β, thereby inhibiting β-catenin stability and affecting the extent of cell proliferation and inflammatory responses.[33] IL-6 is involved in regulating inflammatory responses, immune responses and cell proliferation, among other physiological processes. It can affect inflammatory responses by modulating GSK-3β/β-catenin SPW. The increase in IL-6 may lead to GSK-3β activation, thereby inhibiting β-catenin stability and subsequently influencing extent of cell proliferation and inflammatory responses. These results support the neuroprotective role of ATV in the cerebral hemorrhage model, with its possible mechanisms including the modulation of the GSK-3β/β-catenin SPW, inhibition of inflammatory responses and mitigation of cell damage. It is evident that the potential clinical application of ATV in patients with cerebral hemorrhage should not be underestimated. By inhibiting inflammatory responses and modulating key SPWs, it may play a significant role in protecting neurological function and facilitating recovery. As further research and clinical trials progress, ATV could emerge as one of the effective strategies for treating cerebral hemorrhage.

In summary, ATV inhibits apoptosis of neural cells around hematomas, suppresses inflammation and cell damage by regulating the GSK-3β/β-catenin SPW and improves the experimental cerebral hemorrhage-induced neuroinflammatory response, thus exerting neuroprotective effects. This study elucidates the regulatory mechanism of ATV on neuroinflammatory response after cerebral hemorrhage through the GSK-3β/β-catenin SPW, indicating its potential to inhibit inflammation and cell damage, which is significant for improving the neuroinflammatory response in cerebral hemorrhage rats. However, further analysis is needed in future work regarding the dosage and timing of ATV administration to identify the optimal treatment regimen. Moreover, additional validation of the efficacy and safety of ATV in clinical applications for neuroinflammatory response in cerebral hemorrhage patients is warranted to provide more experimental evidence for its clinical translation. In

summary, ATV demonstrates potential clinical application value in modulating the neuroinflammatory response and providing neuroprotection following cerebral hemorrhage.

CONCLUSION

This work demonstrated the effects of ATV on experimental cerebral hemorrhage and its underlying mechanisms, particularly its relationship with the GSK-3β/β-catenin SPW. The research findings indicate that ATV improves neuroinflammatory response in experimental cerebral hemorrhage rats by modulating the GSK-3β/β-catenin SPW, thereby inhibiting inflammation and cell damage. The neuroprotective effects of ATV in the experimental cerebral hemorrhage model were revealed and its mechanism involving the regulation of GSK-3β/β-catenin SPW was elucidated. These findings provide a theoretical basis for finding novel therapeutic strategies for ICH.

CONFLICT OF INTEREST

The authors declare that there is no conflict of interest.

ABBREVIATIONS

ATV: Atorvastatin; **ICH:** Intracerebral hemorrhage; **SPW:** Signaling pathway; **BWC:** Brain water content; **BT:** Brain tissue; **Ifs:** Inflammatory factors; **TNF:** Tumor necrosis factor; **IL:** Interleukin; **CSF:** Cerebrospinal fluid.

ETHICS APPROVAL AND CONSENT TO PARTICIPATE

The experiment received approval from the Ethical Committee and was conducted in strict compliance with the regulations of the Laboratory Animal Management Regulations concerning all procedures performed on the animals.

SUMMARY

ICH often leads to significant neurological deficits and inflammatory responses and the GSK-3β/β-catenin signaling pathway is closely associated with neuroinflammation and cell damage. ATV has a potential role in neuroprotection, but its effect on post-ICH neuroinflammatory response is not fully understood. The aim of this study was to elucidate the effect of atorvastatin on neuroinflammatory response in rats with experimental cerebral hemorrhage and to investigate its mechanism through the GSK-3β/β-catenin signaling pathway. The effects of ATV on ICH neuroinflammation and GSK-3β/β-catenin signaling pathway were analyzed by constructing ICH model and administering ATV. The results showed that compared with ICH, atorvastatin could increase the neurobehavioral score and regulate the level of GSK-3β/β-catenin signaling pathway protein and the expression of inflammatory factors. It indicated that atorvastatin inhibited the inflammatory response and cell damage after cerebral hemorrhage by regulating the GSK-3β/β-catenin signaling pathway and thus improved the neurological dysfunction and neuroinflammatory response in rats with experimental cerebral hemorrhage. This finding provides a new research basis for the potential application of atorvastatin in neuroprotection after cerebral hemorrhage.

REFERENCES

1. Chen Y, Chen S, Chang J, Wei J, Feng M, Wang R. Perihematomal edema after intracerebral hemorrhage: an update on pathogenesis, risk factors and therapeutic advances. Front Immunol. 2021; 12: 740632. doi: 10.3389/fimmu.2021.740632, PMID 34737745.
2. Sun Y, Li Q, Guo H, He Q. Ferroptosis and iron metabolism after intracerebral hemorrhage. Cells. 2022; 12(1): 90. doi: 10.3390/cells12010090, PMID 36611883.
3. Puy L, Parry-Jones AR, Sandset EC, Dowlatshahi D, Ziai W, Cordonnier C. Intracerebral haemorrhage. Nat Rev Dis Primers. 2023; 9(1): 14. doi: 10.1038/s41572-023-00424-7, PMID 36928219.
4. Zhao S, Liu Z, Yu Z, Wu X, Li R, Tang X. BIO alleviates inflammation through inhibition of GSK-3β in a rat model of intracerebral hemorrhage. J Neurosurg. 2020; 133(2): 383-91. doi: 10.3171/2019.4.JNS183501, PMID 31226691.
5. Yin M, Chen W, Li M, Wang K, Hu N, Li Z. circAFF1 enhances intracerebral hemorrhage induced neuronal ferroptosis by targeting miR-140-5p to regulate GSK-3β mediated Wnt/β-catenin signal pathway. Brain Res Bull. 2022; 189: 11-21. doi: 10.1016/j.brainresbull.2022.08.005, PMID 35952845.
6. Famularo G, Sarrecchia C. Atorvastatin-associated gynecomastia. Ann Pharmacother. 2021; 55(10): 1300-1. doi: 10.1177/1060028021988994, PMID 33472378.
7. Weekman EM, Johnson SN, Rogers CB, Sudduth TL, Xie K, Qiao Q, *et al.* Atorvastatin rescues hyperhomocysteinemia-induced cognitive deficits and neuroinflammatory gene changes. J Neuroinflammation. 2023; 20(1): 199. doi: 10.1186/s12974-023-02883-x, PMID 37658433.
8. Chen D, Sui L, Chen C, Liu S, Sun X, Guan J. Atorvastatin suppresses NLRP3 inflammasome activation in intracerebral hemorrhage via TLR4– and MyD88-dependent pathways. Aging (Albany, NY). 2022; 14(1): 462-76. doi: 10.18632/aging.203824, PMID 35017318.
9. Song Y, Liu X, Yuan J, Sha Z, Jiang W, Liu M, *et al.* Atorvastatin combined with low-dose dexamethasone improves the neuroinflammation and survival in mice with intracerebral hemorrhage. Front Neurosci. 2022; 16: 967297. doi: 10.3389/fnins.2022.967297, PMID 36071715.
10. Ahmad N, Bitar Y, Trefi S. Development and validation of a simple method for the determination of atorvastatin calcium in pure and pharmaceutical formulations using spectrofluorimetry. Heliyon. 2023; 9(3): e13771. doi: 10.1016/j.heliyon.2023.e13771, PMID 36873484.
11. Nakamura S, Saito Y, Gouda T, Imai T, Shimazawa M, Nishimura Y, *et al.* Therapeutic effects of iron chelation in atorvastatin-induced intracranial hemorrhage of zebrafish larvae. J Stroke Cerebrovasc Dis. 2020; 29(11): 105215. doi: 10.1016/j.jstrokecerebrovasdis.2020.105215, PMID 33066911.
12. Yang D, Han Y, Zhang J, Chopp M, Seyfried DM. Statins enhance expression of growth factors and activate the PI3K/Akt-mediated signaling pathway after experimental intracerebral hemorrhage. World J Neurosci. 2012; 2(2): 74-80. doi: 10.4236/wjns.2012.22011, PMID 23482588.
13. Shaghaghi Z, Alvandi M, Farzipour S, Dehbanpour MR, Nosrati S. A review of effects of atorvastatin in cancer therapy. Med Oncol. 2022; 40(1): 27. doi: 10.1007/s12032-022-01892-9, PMID 36459301.
14. Deng S, Feng S, Xin Y, He Y, Wang Y, Tian M, *et al.* Establishment of a rat model of severe spontaneous intracerebral hemorrhage. J Intensive Med. 2024; 4(1): 108-17. doi: 10.1016/j.jointm.2023.08.007, PMID 38263974.
15. Germonpré C, Proesmans S, Bouckaert C, Stevens L, Sprengers M, Vonck K, *et al.* Acute symptomatic seizures following intracerebral hemorrhage in the rat collagenase model. Epilepsy Res. 2020; 164: 106364. doi: 10.1016/j.eplepsyres.2020.106364, PMID 32497986.
16. Qing WG, Dong YQ, Ping TQ, Lai LG, Fang LD, Min HW, *et al.* Brain edema after intracerebral hemorrhage in rats: the role of iron overload and aquaporin 4. J Neurosurg. 2009; 110(3): 462-8. doi: 10.3171/2008.4.JNS17512, PMID 19025353.
17. Tang X, Wu L, Luo M, Qiu Z, Jiang Y. Massive pontine hemorrhage by dual injection of autologous blood. J Vis Exp. 2021; (171): e62089. doi: 10.3791/62089, PMID 34125085.
18. Wilkinson CM, Fedor BA, Aziz JR, Nadeau CA, Brar PS, Clark JJ, *et al.* Failure of bumetanide to improve outcome after intracerebral hemorrhage in rat. PLOS One. 2019; 14(1): e0210660. doi: 10.1371/journal.pone.0210660, PMID 30629699.
19. Liu CZ, Zhou HJ, Zhong JH, Tang T, Cui HJ, Zhou JH, *et al.* Leukemia inhibitory factor decreases neurogenesis and angiogenesis in a rat model of intracerebral hemorrhage. Curr Med Sci. 2019; 39(2): 298-304. doi: 10.1007/s11596-019-2034-2, PMID 31016525.
20. Shirzad S, Vafaee F, Forouzanfar F. The neuroprotective effects and probable mechanisms of everolimus in a rat model of intracerebral hemorrhage. Cell Mol Neurobiol. 2023; 43(8): 4219-30. doi: 10.1007/s10571-023-01409-6, PMID 37747596.

21. Rehni AK, Cho S, Navarro Quero H, Zhang Z, Dong C, Zhao W, *et al.* Red blood cell microparticles limit hemorrhage following intracerebral hemorrhage in spontaneously hypertensive rats. Stroke. 2023; 54(4): e152-4. doi: 10.1161/STROKEAHA.122.042152, PMID 36861474.
22. Gong Y, Deng J, Wu Y, Xu X, Hou Z, Hao S, *et al.* Role of mass effect on neuronal iron deposition after intracerebral hemorrhage. Exp Neurol. 2023; 368: 114475. doi: 10.1016/j.expneurol.2023.114475, PMID 37451583.
23. Deng R, Wang W, Xu X, Ding J, Wang J, Yang S, *et al.* Loss of MIC60 aggravates neuronal death by inducing mitochondrial dysfunction in a rat model of intracerebral hemorrhage. Mol Neurobiol. 2021; 58(10): 4999-5013. doi: 10.1007/s12035-021-02468-w, PMID 34232477.
24. Zhang X, Li H, Hu S, Zhang L, Liu C, Zhu C, *et al.* Brain edema after intracerebral hemorrhage in rats: the role of inflammation. Neurol India. 2006; 54(4): 402-7. doi: 10.4103/0028-3886.28115, PMID 17114852.
25. Yang GY, Betz AL, Hoff JT. The effects of blood or plasma clot on brain edema in the rat with intracerebral hemorrhage. Acta Neurochir Suppl (Wien). 1994; 60: 555-7. doi: 10.1007/978-3-7091-9334-1_153, PMID 7976648.
26. Yu L, Liu S, Zhou R, Sun H, Su X, Liu Q, *et al.* Atorvastatin inhibits neuronal apoptosis via activating cAMP/PKA/p-CREB/BDNF pathway in hypoxic-ischemic neonatal rats. FASEB J. 2022; 36(4): e22263. doi: 10.1096/fj.202101654RR, PMID 35303316.
27. Xu X, Gao W, Cheng S, Yin D, Li F, Wu Y, *et al.* Anti-inflammatory and immunomodulatory mechanisms of atorvastatin in a murine model of traumatic brain injury. J Neuroinflammation. 2017; 14(1): 167. doi: 10.1186/s12974-017-0934-2, PMID 28835272.
28. Yu L, Huang L, Zhao Y, Liu S, Zhou R, Yue Y, *et al.* Atorvastatin promotes pro/anti-inflammatory phenotypic transformation of microglia via Wnt/β-catenin pathway in hypoxic-ischemic neonatal rats. Mol Neurobiol. 2024; 61(6): 3559-77. doi: 10.1007/s12035-023-03777-y, PMID 37996729.
29. Liu C, He P, Guo Y, Tian Q, Wang J, Wang G, *et al.* Taurine attenuates neuronal ferroptosis by regulating GABAB/AKT/GSK3β/β-catenin pathway after subarachnoid hemorrhage. Free Radic Biol Med. 2022; 193(2): 795-807. doi: 10.1016/j.freeradbiomed.2022.11.003, PMID 36402441.
30. Liu J, Liu L, Wang X, Jiang R, Bai Q, Wang G. Microglia: A double-edged sword in intracerebral hemorrhage from basic mechanisms to clinical research. Front Immunol. 2021; 12: 675660. doi: 10.3389/fimmu.2021.675660, PMID 34025674.
31. Xie Y, He W, Ma L, Ren R, Yang S, Lu Q. Endothelial TREM-1 receptor regulates the blood-brain barrier integrity after intracerebral hemorrhage in mice via SYK/β-catenin signaling. CNS Neurosci Ther. 2023; 29(11): 3228-38. doi: 10.1111/cns.14255, PMID 37170484.
32. Wang G, Li Z, Li S, Ren J, Suresh V, Xu D, *et al.* Minocycline preserves the integrity and permeability of BBB by altering the activity of DKK1-Wnt signaling in ICH model. Neuroscience. 2019; 415: 135-46. doi: 10.1016/j.neuroscience.2019.06.038, PMID 31344398.
33. Gu L, Sun M, Li R, Zhang X, Tao Y, Yuan Y, *et al.* Didymin suppresses microglia pyroptosis and neuroinflammation through the ASC/caspase-1/GSDMD pathway following experimental intracerebral hemorrhage. Front Immunol. 2022; 13: 810582. doi: 10.3389/fimmu.2022.810582, PMID 35154128

Cite this article: Zhao J, Li M, Zhang L, Zhang Q. Atorvastatin Ameliorates Neuroinflammatory Response in Experimental Intracerebral Hemorrhage Rats through the GSK-3β/β-Catenin Pathway. Indian J of Pharmaceutical Education and Research. 2025;59(4):1501-10.